

Aging phenomena in critical semi-infinite systems

Michel Pleimling

Institut für Theoretische Physik I, Universität Erlangen-Nürnberg, D – 91058 Erlangen, Germany

Nonequilibrium surface autocorrelation and autoresponse functions are studied numerically in semi-infinite critical systems in the dynamical scaling regime. Dynamical critical behaviour is examined for a nonconserved order parameter in semi-infinite two- and three-dimensional Ising models as well as in the Hilhorst-van Leeuwen model. The latter model permits a systematic study of surface aging phenomena, as the surface critical exponents change continuously as function of a model parameter. The scaling behaviour of surface two-time quantities is investigated and scaling functions are confronted with predictions coming from the theory of local scale invariance. Furthermore, surface fluctuation-dissipation ratios are computed and their asymptotic values are shown to depend on the values of surface critical exponents.

PACS numbers: 64.60.-i, 64.60.Ht, 68.35.Rh, 75.40.Gb

I. INTRODUCTION

Aging behaviour observed in systems with slow degrees of freedom is one of the most intriguing aspects in nonequilibrium physics, see Refs. 1,2,3 for recent reviews. This behaviour is due to relaxation processes which depend on the thermal history of the studied sample. Aging phenomena have been studied extensively in disordered systems like spin glasses or glassy systems, but they are also encountered in the simpler ferromagnetic systems.^{1,4} In the last years remarkable progress has been achieved in our understanding of the physics of aging phenomena taking place in ferromagnets.^{5,6,7,8,9,10,11,12,13,14,15,16,17,18,19,20,21,22,23,24,25,26}

In the typical scenario the ferromagnetic system is prepared in a fully disordered state at high temperatures and then quenched down to temperatures $T \leq T_c$, where $T_c > 0$ is the critical temperature. When the final temperature is smaller than T_c , coarsening takes place, leading to the formation of domains with a time-dependent typical length. It is the slow motion of the domain boundaries which is responsible for the aging processes. The situation is different for a quench to the critical point, where one is dealing with nonequilibrium critical dynamics, as ordered domains do not exist in that case. The typical time-dependent length is then given by the dynamical correlation length $\xi(t) \sim t^{1/z}$, where z is called the dynamical critical exponent.

In recent years investigations concentrated on two-time quantities like dynamical correlation and response functions, as they more fully reveal the aging processes. Examples are the spin-spin autocorrelation function $C(t, s)$ and the conjugate response function $R(t, s)$ defined by

$$C(t, s) = \langle \phi(t)\phi(s) \rangle \quad , \quad R(t, s) = \left. \frac{\delta \langle \phi(t) \rangle}{\delta h(s)} \right|_{h=0} . \quad (1)$$

Here $\phi(t)$ is the time-dependent order parameter, whereas $h(s)$ is the magnetic field conjugate to ϕ . The time t elapsed since the quench is called the observation time and s is referred to as the waiting time. Of course, $R(t, s) = 0$ for $t < s$, due to causality. In the

dynamical scaling regime, $t \gg t_{\text{micro}}$, $s \gg t_{\text{micro}}$ and $\tau = t - s \gg t_{\text{micro}}$, where t_{micro} is some microscopic time, these quantities are expected to have the following behaviour^{1,2}:

$$C(t, s) = s^{-b} f_C(t/s) \quad , \quad R(t, s) = s^{-1-a} f_R(t/s). \quad (2)$$

In the limit $y = t/s \rightarrow \infty$ the scaling functions $f_{C,R}(y)$ present a simple power-law behaviour

$$f_C(y) \sim y^{-\lambda_C/z} \quad , \quad f_R(y) \sim y^{-\lambda_R/z} \quad (3)$$

with the autocorrelation²⁷ and autoresponse¹⁵ exponents λ_C and λ_R . In the case of a quench to the critical point of a ferromagnetic system with initial short-range correlations we have $a = b = 2x/z$ and $\lambda_C = \lambda_R = d - x_i + x$ where d is the number of space dimensions, whereas x resp. x_i denotes the scaling dimension of the order parameter resp. of the initial magnetization.²⁸ A generalization of dynamical scaling to local space-time dependent scaling yields the prediction^{11,14}

$$f_R(y) = r_0 y^{1+a-\lambda_R/z} (y-1)^{-1-a} \quad (4)$$

for the scaling function of the response function $R(t, s)$. This prediction was found to be in excellent agreement with Monte Carlo simulations of two- and three-dimensional Ising models both at and below T_c .^{11,19,20} Similar agreement has recently also been observed for the three-dimensional XY model.²⁶ On the other hand recent renormalization group calculations¹³ yielded at critical points a correction at two loops to the prediction (4) coming from the theory of local scale invariance.¹⁴ The origin of this discrepancy is still not elucidated, but it must be noted that the simulations are based on a master equation, whereas the field theoretical calculations start from a Langevin equation.

Recently, the fluctuation-dissipation ratio

$$X(t, s) = T R(t, s) / \frac{\partial C(t, s)}{\partial s} \quad (5)$$

has attracted much attention in nonequilibrium systems.³ At equilibrium, both $C(t, s)$ and $R(t, s)$

depend only on the time difference $t - s$, and $X(t, s) = 1$, thus recovering the well-known fluctuation-dissipation theorem. However, this is not the case far from equilibrium where $X(t, s) \neq 1$. This property led to numerous studies of $X(t, s)$ in various systems with the aim to possibly quantify the distance to equilibrium. In the context of glassy systems the limit value X^∞ has been interpreted as giving rise to an effective temperature $T_{eff} = T/X^\infty$.²⁹ Godrèche and Luck conjectured that in critical systems the asymptotic value $X^\infty = \lim_{s \rightarrow \infty} \left(\lim_{t \rightarrow \infty} X(t, s) \right)$ of this nonequilibrium quantity characterizes the different universality classes.⁹ This has indeed been confirmed in exactly solvable cases,^{8,10,30} in various Monte Carlo studies^{1,9,16,17,25,31} as well as in field-theoretical calculations.¹³

Surfaces are unavoidable in real materials and play an outstanding role in nanotechnologies. It is therefore of importance to understand the local behaviour close to a surface in nonequilibrium systems. In this work we take a step in that direction and extend the investigation of aging phenomena in critical systems to the semi-infinite geometry, focusing on aging processes taking place in the vicinity of the surface.

It is well known that the presence of symmetry-breaking surfaces changes local quantities, leading to surface critical behaviour which differs from that of the bulk (see Refs. 32,33 for recent reviews). For example, the static critical surface pair correlation function behaves as $|\vec{\rho} - \vec{\rho}'|^{-2x_1}$, where for a d -dimensional model $\vec{\rho}$ is a $(d - 1)$ -dimensional vector parallel to the surface. The scaling dimension x_1 of the surface order parameter differs in general from the scaling dimension x of the bulk order parameter. Of further importance is the fact that, depending on the surface interactions, different surface universality classes may be realized for a given bulk universality class. An important case is that of the three-dimensional semi-infinite Ising model where three different surface universality classes are encountered at the bulk critical temperature.

The present work studies the effect of surfaces on aging processes with a non-conserved order parameter in the dynamical scaling regime $t, s \gg t_{micro}$, $t - s \gg t_{micro}$. We thereby discuss not only two- and three-dimensional semi-infinite Ising models, but also analyze aging phenomena taking place in the Hilhorst-van Leeuwen model.^{34,35} The latter model is a semi-infinite two-dimensional Ising model with an extended surface defect. In this model the surface scaling dimension x_1 has been shown to vary continuously as a function of the defect amplitude in the interesting case that the surface defect is a marginal perturbation. This makes it possible to systematically study at criticality the impact of surfaces on local two-time correlation and response functions as well as on related quantities as local fluctuation-dissipation ratios.

This work is also meant to close a gap in the study of critical dynamics at surfaces. Prior works either treated

equilibrium critical dynamics near surfaces^{36,37,38} or focused mainly on the effect a surface has on nonequilibrium critical dynamics immediately after the quench to the critical point.^{39,40,41,42,43} To our knowledge the dynamical scaling regime has not yet been investigated in semi-infinite critical systems.

The paper is organized in the following way. In Section II the different semi-infinite models are introduced and some important facts on equilibrium and dynamic surface critical behaviour are reviewed. Section III deals with surface two-time autocorrelation functions in the dynamical scaling (i.e. aging) regime, whereas Section IV is devoted to the corresponding study of the thermoremanent magnetization. These quantities are examined in the Hilhorst-van Leeuwen model for various values of the defect amplitude. In the three-dimensional semi-infinite Ising model, both the ordinary transition (where the bulk alone is critical) and the special transition point (where bulk and surface are both critical) are considered. In Section IV numerically determined scaling functions derived from the integrated responses are compared with predicted scaling functions coming from the theory of local scale invariance. Section V is devoted to the analysis of surface fluctuation-dissipation ratios. It is shown that the limit value of this ratio depends on the value of the surface scaling dimension x_1 . Interpreting this asymptotic value as giving rise to an effective temperature, it follows that for a given bulk universality class different surface effective temperatures may be obtained by varying the value of some local model parameters. Finally, Section VI gives our conclusions as well as an outlook on open problems.

II. CRITICAL BEHAVIOUR NEAR SURFACES

A. Models and surface phase diagrams

All the models studied in this work are defined on d -dimensional semi-infinite (hyper)cubic lattices. Every lattice point is characterized by an Ising spin which takes on the values ± 1 . For the pure, perfect Ising model in absence of external fields, the Hamiltonian is given by

$$\mathcal{H} = -J_b \sum_{bulk} \sigma_i \sigma_j - J_s \sum_{surface} \sigma_i \sigma_j. \quad (6)$$

The first sum is over nearest neighbour pairs where at most one spin is a surface spin, whereas the second sum is over nearest neighbour pairs with both spins lying in the surface layer. J_b resp. J_s is the strength of the bulk resp. surface couplings. All couplings are supposed to be ferromagnetic, i.e. $J_b, J_s > 0$.

The surface phase diagrams of the two- and three-dimensional semi-infinite Ising models (6) are well established.^{32,33} In two dimensions only one surface universality class, the so-called ordinary transition, is encountered at the bulk critical point for all values of the

surface couplings. This transition is characterized by the value $x_1 = 1/2$ of the scaling dimension of the surface order parameter. Here and in the following I follow the usual convention and characterize surface quantities by the index 1. The surface phase diagram is more interesting for the three-dimensional model. If the ratio of the surface coupling J_s to the bulk coupling J_b , $r = J_s/J_b$, is sufficiently small, the system undergoes at the bulk critical temperature T_c an ordinary transition, with the bulk and surface orderings occurring at the same temperature. Beyond a critical ratio, $r > r_{sp} \approx 1.50$ for the semi-infinite Ising model on the simple cubic lattice,^{44,45} the surface orders at the so-called surface transition at a temperature $T_s > T_c$, followed by the extraordinary transition at T_c . At the critical ratio r_{sp} , one encounters the multicritical special transition point, with critical surface properties deviating from those at the ordinary transition and those at the surface transition. The present work exclusively treats aging processes taking place at the ordinary transition and at the special transition point. For these cases the scaling dimension x_1 takes on the values 1.26 (ordinary transition) and 0.376 (special transition point).

The Hilhorst-van Leeuwen model^{34,35} is a critical two-dimensional semi-infinite Ising model with an extended surface defect due to inhomogeneous couplings. Considering a square lattice, one has couplings with a constant strength J_1 in the direction parallel to the surface, whereas the strength of the couplings varies perpendicular to the surface as a function of the distance l to the surface:

$$J_2(l) - J_2(\infty) = \frac{\tilde{A}}{l^\omega}. \quad (7)$$

with $\tilde{A} = AT_c \sinh(2J_2(\infty)/T_c)/4$.⁴⁶ In this work J_1 is set equal to $J_2(\infty)$. This extended perturbation is irrelevant for $\omega > 1$, yielding the same critical behaviour as the homogeneous semi-infinite system. For $\omega < 1$ and $A > 0$, however, the perturbation is relevant and a spontaneous surface magnetisation is observed at the bulk critical point. In the present context the most interesting case is obtained for $\omega = 1$, where the perturbation is marginal for $A < 1$ (for $A > 1$ one again observes a spontaneous surface magnetisation). Indeed, exact results show that the scaling dimension x_1 is then a continuous function of the parameter A with

$$x_1 = \frac{1}{2}(1 - A) \quad (8)$$

and $A < 1$. This intriguing behaviour, which has attracted much interest in the past, gives us the possibility to continuously change the surface critical exponents for a given bulk universality class (that of the two-dimensional Ising model), thereby making a systematic study of aging processes at critical surfaces possible.

TABLE I: Literature values of bulk and surface scaling dimensions x and x_1 as well as of the nonequilibrium dynamical bulk exponents x_i and z , for both the two- and the three-dimensional Ising models. OT: ordinary transition, SP: special transition point.

	x	x_1	x_i	z
$d = 2$	1/8	1/2	0.53	2.17
$d = 3$, OT	0.516	1.26	0.74	2.04
$d = 3$, SP	0.516	0.376	0.74	2.04

B. Critical dynamics near surfaces

Besides changing the local static critical behaviour, surfaces have also an effect on critical dynamics. This has been studied in semi-infinite extensions of the well-known bulk stochastic models,⁴⁷ as for example model A (purely relaxational without any conserved quantities)^{36,37} or model B (with conserved order parameter).^{37,48} A central aspect of the works on dynamic surface critical behaviour concerns the possible classification of the distinct surface dynamic universality classes.

It is important to note that no genuine dynamic surface exponent exists.^{36,39} All exponents describing the surface critical behaviour of dynamic quantities can be expressed entirely in terms of static bulk and surface exponents and the dynamic bulk exponents z and x_i . The values of the critical exponents that are of interest in the following are listed in Table I for the two- and the three-dimensional Ising models. Consider as an example the dynamic surface spin-spin autocorrelation function. At equilibrium it decays for long times as $t^{-2x_1/z}$,³⁶ whereas out-of-equilibrium one expects from scaling arguments and field-theoretical calculations the power-law behaviour $t^{-\lambda_1/z}$ with the surface autocorrelation exponent

$$\lambda_1 = \lambda_C + 2(x_1 - x) \quad (9)$$

and $t \gg 1$ being the time elapsed since the quench.^{39,40} This prediction has up to now only been verified in semi-infinite Ising models.

Out-of-equilibrium studies of dynamic surface critical behaviour are very scarce.^{39,40,41,42,43} In Ref. 39 short-time critical relaxation was analysed at surfaces by preparing the system at high temperatures with a small initial surface magnetization. As in the bulk case, a power-law behaviour of the surface magnetization is observed at early times, governed by the nonequilibrium exponent $\theta_1 = (x_i - x_1)/z$. Recently the two-time surface autocorrelation function $C_1(t, s)$ was analysed in the short-time regime $t - s \ll s$.⁴³ Using scaling arguments it was predicted that in the case $x_i < x_1$ a new effect, called cluster dissolution, takes place, which should lead to an unconventional, stretched exponential dependence of the short-time autocorrelation:

$$C_1(t - s) \sim \exp(-\overline{C}(t - s)^\kappa) \quad (10)$$

with

$$\kappa = \frac{(x_1 - x_i)d}{z(d-1)}. \quad (11)$$

It follows that for $t - s \ll s$ a stationary behaviour should be observed, as the autocorrelation in this case only depends on the time difference $t - s$. These predictions were verified by simulating the dynamical evolution of the Hilhorst-van Leeuwen model for various values of x_1 . Interestingly, this stretched exponential behaviour is also observed in the three-dimensional semi-infinite Ising model at the ordinary transition⁴³ where $x_i = 0.74$ and $x_1 = 1.26$. For the case $x_i > x_1$, on the other hand, no stationary behaviour is predicted for $t - s \ll s$. It is worth noting that dynamical surface response functions have not yet been analyzed in critical semi-infinite systems.

In the dynamical scaling regime ($t, s, t - s \gg t_{micro}$) it is expected that the surface autocorrelation function $C_1(t, s)$ and the surface autoresponse function $R_1(t, s)$ exhibit a behaviour similar to that of the corresponding bulk quantities, but with surface exponents replacing the bulk exponents:

$$C_1(t, s) = s^{-b_1} f_{C_1}(t/s) \quad (12)$$

$$R_1(t, s) = s^{-1-a_1} f_{R_1}(t/s) \quad (13)$$

The scaling functions $f_{C_1}(y)$ and $f_{R_1}(y)$ display again a power-law behaviour in the limit $y \rightarrow \infty$:

$$f_{C_1}(y) \sim y^{-\lambda_C^1/z}, \quad f_{R_1}(y) \sim y^{-\lambda_R^1/z}. \quad (14)$$

In the case of a quench to a critical point from an initially uncorrelated state, one expects

$$\lambda_C^1 = \lambda_R^1 = \lambda_1 \quad (15)$$

where λ_1 is given by Eq. (9). Furthermore, one should have that³⁶

$$a_1 = b_1 = 2x_1/z \quad (16)$$

where x_1 is again the surface scaling dimension.

III. SURFACE AUTOCORRELATION IN THE AGING REGIME

The scaling behaviour (12) of the surface autocorrelation function is predicted to be valid in the dynamical scaling regime for all values of x_1 . In the short-time regime, however, one has to distinguish whether $x_i > x_1$, so that the usual domain growth mechanism prevails (this is the same situation as encountered in bulk systems), or whether $x_i < x_1$, in which case cluster dissolution takes place,⁴³ leading to the stationary stretched exponential behaviour (10). In the domain growth regime, the scaling form (12) is expected to be valid even for $t - s < s$.

These predictions are confronted in the following with results obtained in extensive Monte Carlo simulations of the Hilhorst-van Leeuwen model and of the three-dimensional semi-infinite Ising model. For the former model, various values of the amplitude A were considered, with the value of the scaling dimension of the surface magnetization ranging from $x_1 = 1/4$ to $x_1 = 1$, see Eqs. (7) and (8). The homogeneous two-dimensional semi-infinite Ising model is recovered in the special case $A = 0$ and $x_1 = 1/2$. The different systems were prepared at $t = 0$ at infinite temperature (i.e. completely uncorrelated initial state) and then quenched down to the critical point. Applying heat-bath dynamics, the dynamical evolution of the system was studied for times $t > 0$. Heat-bath dynamics was chosen so that no macroscopic quantities were conserved. After the waiting time s the time dependence of the dynamical surface autocorrelation function $C_1(t, s)$ was measured, with

$$C_1(t, s) = \frac{1}{N} \sum_{i \in \text{surface}} \langle \sigma_i(t) \sigma_i(s) \rangle \quad (17)$$

and $t > s$. The sum in (17) is over all surface spins, N is the total number of surface sites, whereas $\sigma_i(t)$ is the value of the spin located at the surface site i at time t . The brackets indicate an average over thermal noise. Typically, the average has been taken over more than 10000 different realizations with different random numbers. In the actual simulations, systems with 300×300 spins were simulated in two dimensions, with periodic boundary condition in the direction parallel to the surfaces and free boundary condition in the non-homogeneous direction. For the three-dimensional Ising model, systems with typically 40 layers with 60×60 spins per layer were studied. Here, periodic boundary conditions were used in both directions parallel to the surfaces. In both cases some simulations for other system sizes were also done, in order to check against finite-size effects. All the data discussed in this work are free from this kind of effects.

Figure 1 gives a first impression of the impact that the surface scaling dimension x_1 has on the surface two-time autocorrelation function. The Figure displays autocorrelation functions obtained in the Hilhorst-van Leeuwen model for various values of x_1 , ranging from $x_1 = 1/4$ (top) to $x_1 = 1$ (bottom), with the waiting time fixed at $s = 25$. The grey dashed line is the function obtained for $A = 0$, i.e. for the homogeneous two-dimensional semi-infinite Ising model. The data show that when the value of x_1 increases, the decay of the correlation becomes faster. This is due to two different effects: (a) in the long-time limit, the scaling function $f_{C_1}(t/s)$, which is proportional to $C_1(t, s)$, displays a power-law decay with the exponent λ_1/z , where λ_1 increases with x_1 (see Eq. (9)), and (b) at short times with $x_1 > x_i$, the initial behaviour is that of a stretched exponential where the exponent κ again increases with x_1 ,⁴³ see Eq. (11).

The scaling function $f_{C_1}(t/s) = s^{2x_1/z} C_1(t, s)$ is shown in Figure 2 for three different values of the scal-

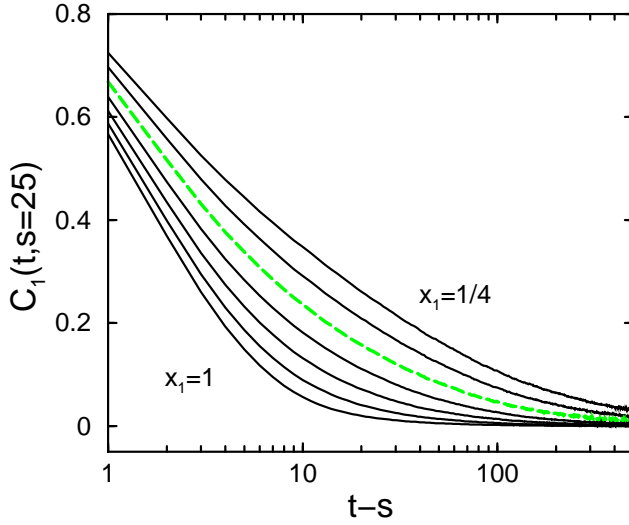


FIG. 1: Dynamical surface spin-spin autocorrelation functions vs $t - s$ for s fixed at 25, as obtained in the Hilhorst-van Leeuwen model. The different curves correspond to different values of the surface scaling dimension: $x_1 = 1/4, 3/8, 1/2, 5/8, 3/4, 7/8, 1$ (from top to bottom). The dashed grey line is obtained for the pure homogeneous two-dimensional Ising model with $x_1 = 1/2$.

TABLE II: Comparison of numerically determined values of λ_1/z with the theoretical expectations (9). λ_1/z has been determined from both the autocorrelation (C) and the autoreponse (R) functions. The errors result from averaging over different waiting times. The available numerical data do not permit to reliably determine λ_1/z for $x_1 > 3/4$ in the case of the Hilhorst-van Leeuwen model. HvL: Hilhorst-van Leeuwen model, OT: ordinary transition, SP: special transition point.

HvL	A	x_1	expected	$\lambda_1/z(C)$	$\lambda_1/z(R)$
	0.50	1/4	0.85	0.84(1)	0.84(1)
	0.25	3/8	0.96	0.96(1)	0.95(1)
	0	1/2	1.08	1.09(1)	1.12(2)
	-0.25	5/8	1.19	1.22(2)	1.21(2)
	-0.50	3/4	1.31	1.30(2)	1.35(3)
$d = 3$	OT	1.26	2.10	2.10(1)	2.18(3)
$d = 3$	SP	0.376	1.22	1.16(2)	1.24(2)

ing dimension x_1 . In all cases a perfect data collapse is achieved when plotting $f_{C_1}(t/s)$ for different waiting times. As $x_1 > x_i$ for $x_1 = 3/4$, one has in that case a stationary stretched exponential behaviour at early times,⁴³ and therefore the scaling is not expected to work at short times. This is indeed the case, but this effect is not visible on the scale used in Figure 2 (see, however, the inset in Figure 4 below). The range of waiting times shown here is comparable to that of Ref. 11, where aging processes taking place in critical bulk systems were investigated. The dashed lines illustrate the expected long-time behaviour (14) of the scaling function, which is in com-

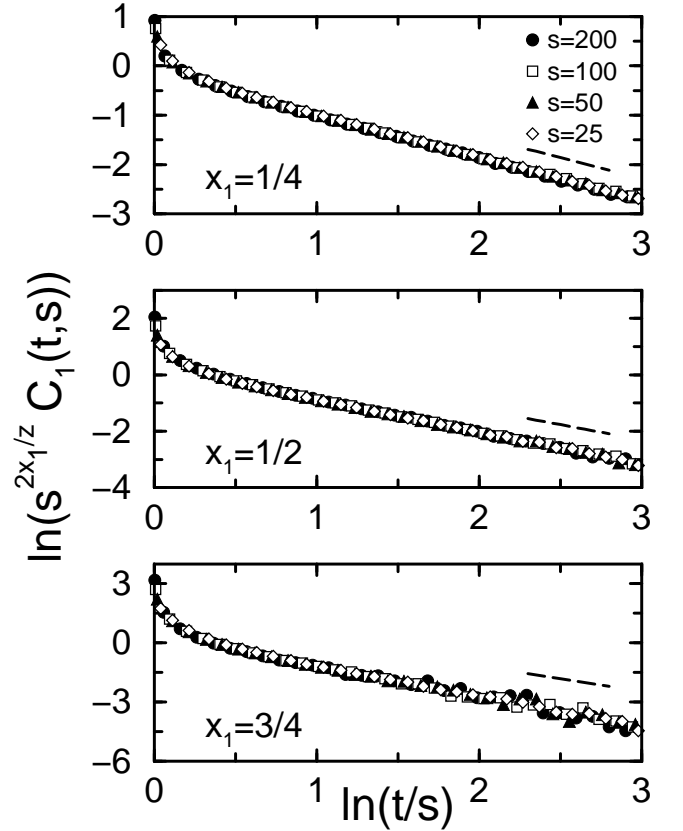


FIG. 2: Logarithm of the scaling function $f_{C_1}(t/s) = s^{2x_1/z} C_1(t, s)$ as function of the logarithm of the scaling variable t/s . The data shown have been obtained in the Hilhorst-van Leeuwen model for three different values of the surface scaling dimension x_1 and various waiting times s . The dashed lines indicate the expected power-law behaviour for $t/s \gg 1$. Here and in the following, errors are comparable to the scattering of the data.

plete agreement with the numerical data, see Table II. Unfortunately, no theoretical prediction of the complete functional form of the scaling function exists. There has been some recent progress in the derivation of an analytical expression for f_C in the bulk system,^{24,49} but these achievements are up to now only applicable to the special case $z = 2$ not realized in the critical systems we are interested in.

In the three-dimensional semi-infinite Ising model different surface universality classes are encountered when changing the strength J_s of the surface couplings. This is not the case in two dimensions, where one has only the ordinary transition for all values of J_s . Nevertheless, the dynamical two-time autocorrelation function is affected by a change of the value of J_s . This is illustrated in Figure 3 where the logarithm of the scaling function is plotted for three different values of $r = J_s/J_b$: $5/4, 1, 3/4$, and two different waiting times. One remarks that $C_1(t, s)$ decreases with increasing value of r for a given value of t/s . However, when multiplying $C_1(t, s)$

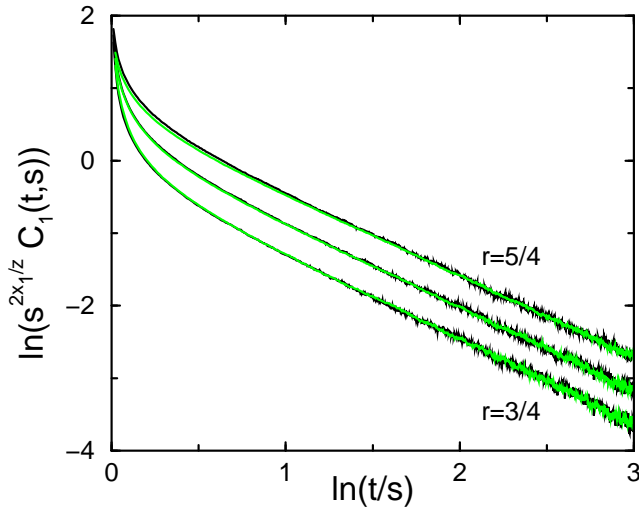


FIG. 3: Logarithm of the scaling function $f_{C_1}(t/s) = s^{2x_1/z} C_1(t,s)$ obtained in the two-dimensional semi-infinite Ising model as function of $\ln(t/s)$ for three different values of the strength $J_s = r J_b$ of the surface couplings, with $r = 5/4$ (top), 1, and $3/4$. The black (grey) lines correspond to waiting times $s = 100$ (50).

by a constant so that the different curves coincide for large values of t/s , one observes that the rescaled functions are identical in the whole aging regime. It is only at short times with $t - s < s$ that slight deviations are observed. This is not surprising, as the short-time behaviour of the dynamical autocorrelation function is not expected to be universal in the present case. Concerning the aging regime, one may conclude that the scaling law (12) should in fact read

$$C_1(t,s) = \Omega(J_s) s^{-2x_1/z} f_{C_1}(t/s) \quad (18)$$

where only the amplitude Ω depends on the strength J_s of the surface couplings. The same conclusion holds for values of $A \neq 0$.

Finally, Figure 4 shows the scaling functions f_{C_1} determined in the semi-infinite three-dimensional Ising model for two different surface universality classes: the ordinary transition (with $J_s = J_b$) and the special transition point (with $J_s = 1.5J_b$). In both cases data collapse is achieved when inserting the correct values of the surface scaling dimension, see Table I. The inset illustrates the short-time behaviour. Recall that at the ordinary transition $x_1 = 1.26 > x_i$, whereas at the special transition point $x_1 = 0.376 < x_i$. Following the scaling arguments given above, a stationary behaviour is expected in the former case, yielding at short times deviations from the scaling behaviour (12), whereas in the latter case the same scaling behaviour should also prevail at short times. This is indeed what is observed.

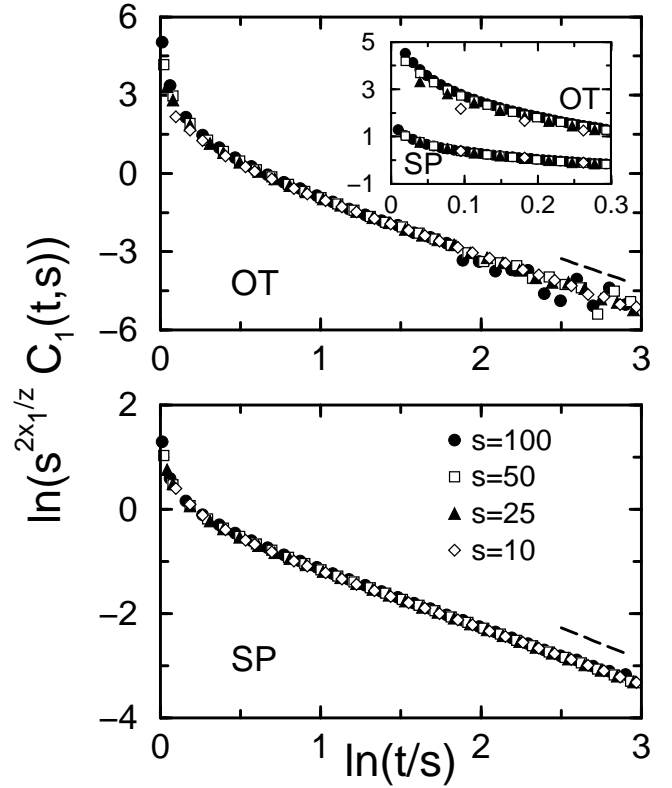


FIG. 4: The same as Figure 2, but now for the three-dimensional Ising model at the ordinary transition (OT) and at the special transition point (SP). The dashed lines indicate again the expected power-law behaviour for $t/s \gg 1$. Inset: short-time behaviour showing the predicted deviations from scaling at the ordinary transition, whereas at the special transition point the scaling behaviour (12) is also observed at short times.

IV. SURFACE THERMOREMANENT MAGNETIZATION

In order to compute the surface thermoremanent magnetization we follow Barrat⁶ and prepare the system in an uncorrelated initial state before quenching it down to the critical point in presence of a small binary random field $h_i = \pm h$. After the waiting time s the field is switched off and the surface (staggered) magnetization

$$M_1(t,s) = \frac{1}{N} \sum_{i \in \text{surface}} \overline{\langle h_i \sigma_i(t) \rangle} / T_c \quad (19)$$

is measured, with $t > s$ being the time elapsed since the quench. Here $\langle \dots \rangle$ indicates again an average over the thermal noise whereas the bar means an average over the random field distribution. The sum in Eq. (19) is restricted to the N surface sites.

It is very expensive to obtain good data for the surface integrated response function at larger values of the ratio t/s . This is due to the value of the surface scaling dimension, which governs to a large extent the behaviour in the

aging regime and which in general considerably exceeds the value of the scaling dimension in the bulk. In the simulations I went up to observation times $t = 21$ s and typically averaged over 500000 different realizations for every waiting time considered. The sizes of the systems are the same as those used for the study of the surface autocorrelation function.

The local thermoremanent magnetization is related to the surface response function by

$$M_1(t, s) = h \int_0^s du R_1(t, u). \quad (20)$$

$M_1(t, s)$ should have the following scaling behaviour in the dynamical scaling regime

$$M_1(t, s)/h = s^{-2x_1/z} f_{M_1}(t/s) \quad (21)$$

with the scaling function f_{M_1} . Expression (21) results from inserting the expected behaviour (13) of the surface response function into Eq. (20).

Exact expressions for the scaling functions f_{R_1} and f_{M_1} are obtained by assuming that local scale invariance^{11,14} holds. As shown in the Appendix, one then obtains for the surface autoresponse the expression

$$f_{R_1}(y) = r_0 y^{1+2x_1/z-\lambda_1/z} (y-1)^{-1-2x_1/z} \quad (22)$$

and, after integration,

$$f_{M_1}(y) = r_0 y^{-\lambda_1/z} {}_2F_1(1+2x_1/z, \lambda_1/z-2x_1/z; \lambda_1/z-2x_1/z+1; y^{-1}) \quad (23)$$

where ${}_2F_1$ is a hypergeometric function. Expressions (22) and (23) are similar to those obtained for bulk systems,¹⁴ but now the surface scaling dimension x_1 and the surface autoresponse exponent λ_1 replace the corresponding bulk quantities.

The scaling form (21) results by naively inserting Eq. (13) into Eq. (20) without taking into account that the condition for the validity of (13) is violated at the lower integration bound. It was shown in¹⁹ that in case the system undergoes phase-ordering at temperatures below T_c the leading correction-to-scaling term can usually not be neglected. However, at a critical point this correction term, which is of the form $s^{-\lambda_1/z} g_{M_1}(t/s)$,¹⁹ where g_{M_1} is a scaling function known in the framework of the theory of local scale invariance, should not have a sizeable effect, as λ_1/z is much larger than $2x_1/z$. (In case of a bulk system, the local exponents λ_1 and x_1 have of course to be replaced by the corresponding bulk exponents.) This has been confirmed in the study of aging phenomena in critical bulk systems,¹¹ and it is also the case for the surface thermoremanent magnetization discussed in the following.

The behaviour of the autoresponse function in the short-time regime $t-s < s$ has not yet been discussed in the literature. Some conclusions regarding the autoresponse function may, however, be drawn by remarking

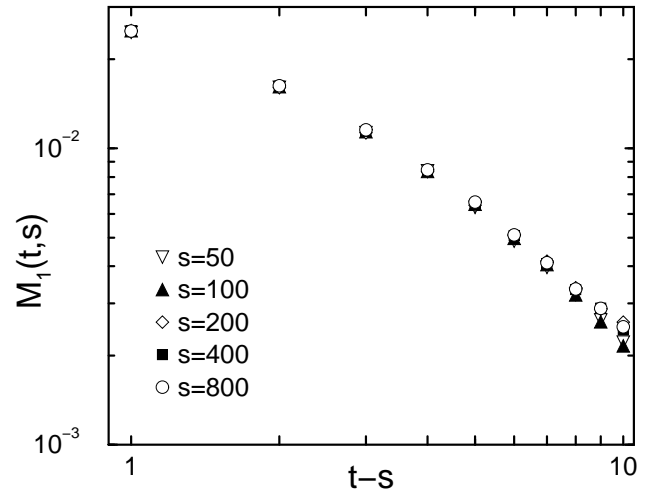


FIG. 5: The thermoremanent magnetization as function of the time difference $t-s$ in the Hilhorst-van Leeuwen model with $x_1 = 1$ and $h = 0.1$. A stationary regime is observed at early times as $M_1(t, s)$ only depends on $t-s$. In this figure error bars are comparable to the symbol sizes.

that for $t-s \ll s$ the system is in local equilibrium, yielding a fluctuation-dissipation ratio $X(t, s)$, see (5), that takes on its equilibrium value 1.³ This ratio shows strong deviations from its equilibrium behaviour only at later times when leaving the quasiequilibrium regime, as discussed in the next Section. It may therefore be concluded that the autoresponse function should exhibit at short times a stationary behaviour every time the autocorrelation function displays this kind of behaviour. This is indeed the case, as illustrated in Figure 5 for the Hilhorst-van Leeuwen model with $x_1 = 1$.

The main findings of this Section are summarized in Figures 6 and 7, showing the rescaled thermoremanent magnetization in the Hilhorst-van Leeuwen model for different values of the surface scaling dimension as well as in the three-dimensional Ising model at the ordinary transition and at the special transition point. One remarks that in all cases the thermoremanent magnetization shows a perfect scaling behaviour and that the scaling function $f_{M_1}(t, s) = s^{2x_1/z} M_1(t, s)$ for $t-s > s$ indeed only depends on the scaling variable t/s . Deviations from scaling are observed for $t-s < s$ when $x_i < x_1$, as expected. The scattering of the data in these figures being a measure of the error bars, it is obvious that reliable data are more difficult to obtain for larger values of x_1 . This fact precludes the study of the autoresponse function in the aging regime for values of x_1 much larger than 1.

The full lines in Figures 6 and 7 are obtained from the theoretical prediction (23) by inserting the numerical values of the scaling dimensions x_1 and x_i . The non-universal amplitude r_0 has thereby been fixed by requiring that the analytical curve and the numerical data coincide for large values of t/s . In cases where $x_i > x_1$ the theoretical curves perfectly describe the numerical data over

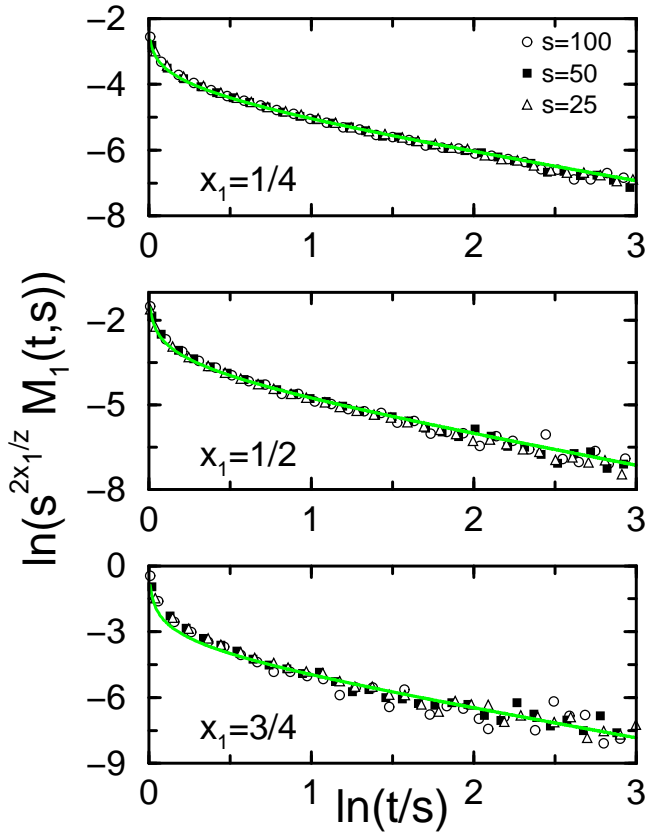


FIG. 6: Logarithm of the scaling function of the thermoremanent magnetization as function of $\ln(t/s)$, as obtained in the Hilhorst-van Leeuwen model for three different values of the surface scaling dimension x_1 and for different waiting times. The strength of the binary random field was $h = 0.1$. The full grey lines follow from the theoretical prediction (23).

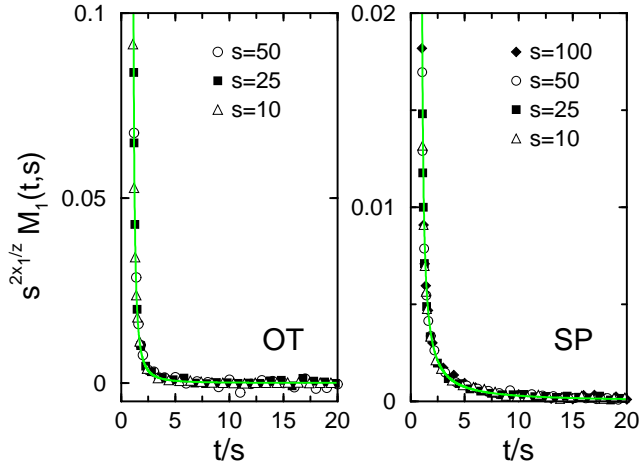


FIG. 7: The scaling function of the thermoremanent magnetization vs t/s , as obtained in the three-dimensional semi-infinite Ising model at the ordinary transition (OT) with $J_s = J_b$ and at the special transition point (SP), with $h = 0.05$. The full grey lines are the theoretical predictions (23) coming from the theory of local scale invariance.

the whole range of values of the ratio t/s . Deviations are observed in the short-time regime $t - s < s$ when $x_i < x_1$. This is obvious in Figure 6 for $x_1 = 3/4$, but it is also the case for the three-dimensional Ising model at the ordinary transition, as revealed by scrutinizing more closely the early time behaviour. These deviations are of course due to the fact that for $t - s \ll s$, i.e. outside of the dynamical scaling regime, the surface autoresponse (and therefore also the thermoremanent magnetization) exhibits a stationary behaviour. However, even in these cases the analytical curve again nicely match the numerical data for $t - s > s$.

The situation at the surface is therefore similar to that encountered inside the bulk:¹¹ in both cases no systematic deviations from the theoretical prediction coming from the theory of local scale invariance are observed in the aging regime when analyzing the numerical data. This is a remarkable result, as it indicates that the scaling function of the autoresponse is completely fixed when knowing the values of two critical exponents: the scaling dimension x_l of the local order parameter (x_l being equal to x resp. x_1 inside the bulk resp. close to the surface) and the scaling dimension x_i of the initial magnetization. At this stage one has to remember, however, that renormalization group calculations¹³ yield in the bulk system a correction to the predicted behaviour (4) at two loops. Similar corrections are then also expected in a field-theoretical treatment of the surface response function in semi-infinite systems. It is an open problem why these corrections are not directly revealed when comparing the numerical data with the local scale invariance prediction. An obvious explanation would of course be that these corrections are in fact very small and therefore difficult to observe. There may, however, also be hidden a more fundamental problem. Indeed, exact results in one dimension yield the value $\lambda_C = 1$ for the Glauber-Ising model at the critical point $T = 0$,⁵⁰ whereas one obtains from the time-dependent Ginzburg-Landau equation,⁵¹ which is usually thought to describe the same system, the value $\lambda_C = 0.6006$. This indicates that the one-dimensional Glauber-Ising model and the time-dependent Ginzburg-Landau equation belong to different universality classes, which leaves open the possibility that similar problems arise in higher dimensions.⁵² Clearly, further investigations are called for in order to clarify this important issue.

Before coming to the surface fluctuation-dissipation ratio in the next Section, let me briefly comment on the range of waiting times accessed in the present study. Indeed, a reader familiar with the investigations of aging phenomena in spin glasses may be surprized by the apparently small values of s retained here. In critical ferromagnets the decay of, for example, the thermoremanent magnetization is very fast, due to the large values of λ_R/z (being for the three-dimensional Ising model 1.73 in the bulk and 2.10 at the surface), whereas in spin glasses the decay is much slower with λ_R/z typically of the order of $0.1 - 0.4$. This slow decrease makes it possible to access

much longer waiting times in spin glasses. On the other hand, however, the dynamical scaling regime is entered for spin glasses only for large values of s , whereas in ferromagnets dynamical scaling behaviour is already observed for rather small values of s , as illustrated for instance in the different figures discussed in this work.

V. SURFACE FLUCTUATION-DISSIPATION RATIOS

One of the central quantity in the study of systems far from equilibrium is the fluctuation-dissipation ratio $X(t, s)$ given by Eq. (5).³ In the context of critical systems one is especially interested in the limiting value

$$X^\infty = \lim_{s \rightarrow \infty} \left(\lim_{t \rightarrow \infty} X(t, s) \right) \quad (24)$$

which characterizes the different universality classes.^{9,13} For example, one obtains in the case of Glauber dynamics the value $X^\infty = 0.33$ for the two-dimensional Ising model,^{16,17} whereas in three dimensions one has $X^\infty \approx 0.4$.⁹ In the exactly solvable one-dimensional case this value is $X^\infty = 1/2$ at $T = 0$,^{8,10} when starting from an uncorrelated initial state.³⁰ This limiting value can also be obtained from the thermoremanent magnetization.⁹ Indeed, in the scaling limit the scaling functions f_C and f_R of the autocorrelation and response functions only depend on t/s , yielding $M(t, s) = M(C(t, s))$ and therefore⁹

$$X^\infty = \lim_{C \rightarrow 0} \frac{T_c M(C)}{h C}. \quad (25)$$

Fluctuation-dissipation ratios have up to now only been studied in bulk systems.

We define the surface fluctuation-dissipation ratio in complete analogy to the bulk case, but with surface quantities replacing the bulk ones:

$$X_1(t, s) = T_c R_1(t, s) / \frac{\partial C_1(t, s)}{\partial s} \quad (26)$$

The limiting value of the surface fluctuation-dissipation ratio is then given by the expression

$$X_1^\infty = \lim_{C_1 \rightarrow 0} \frac{T_c M_1(C_1)}{h C_1}. \quad (27)$$

where C_1 and M_1 are the surface autocorrelation function and the surface thermoremanent magnetization studied in the preceding Sections.

Figures 8a and 8b display the parametric plot of the rescaled thermoremanent magnetization $s^{2x_1/z} T_c M_1/h$ versus the rescaled autocorrelation function $s^{2x_1/z} C_1$ for two different cases: the pure two-dimensional semi-infinite Ising model and the semi-infinite three-dimensional Ising model at the special transition point. In both cases the data points for different waiting times show the expected perfect scaling. A similar good

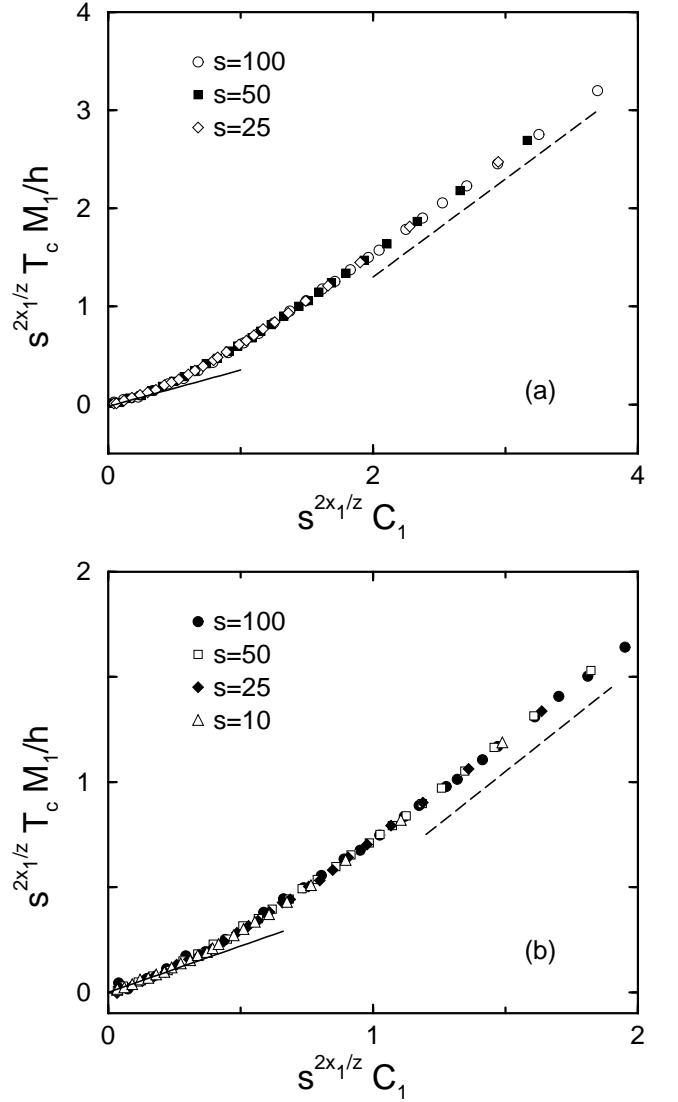


FIG. 8: The rescaled surface thermoremanent magnetization versus the rescaled autocorrelation function: (a) perfect two-dimensional semi-infinite Ising model with $A = 0$ and (b) the three-dimensional semi-infinite Ising model at the special transition point. The dashed lines indicates the quasiequilibrium regime at early times, whereas the slope of the full lines is given by the limiting value X_1^∞ of the surface fluctuation-dissipation ratio, see Eq. (25) and Table III.

scaling is observed for all studied systems in two and three dimensions. At early times, $t - s \ll s$, a quasiequilibrium behaviour, where the fluctuation-dissipation theorem holds, is indeed observed, as indicated by the dashed lines with slope 1. In the limit $C_1 \rightarrow 0$ the slope of these parametric plots yield the asymptotic values X_1^∞ of the surface fluctuation-dissipation ratios, as indicated by the full lines. Alternatively, one may also investigate X_1 as function of s/t , which yields the limit value X_1^∞ for $s/t \rightarrow 0$. Both approaches give comparable results. The limiting values determined for the

TABLE III: The limiting value X_1^∞ of the fluctuation-dissipation ratio obtained from Eq. (25) for the different models. HvL: Hilhorst-van Leeuwen model, OT: ordinary transition, SP: special transition point.

HvL	A	x_1	X_1^∞
	0.50	1/4	0.31(1)
	0.25	3/8	0.33(1)
	0	1/2	0.37(1)
	-0.25	5/8	0.40(2)
	-0.50	3/4	0.43(2)
$d = 3$	OT	1.26	0.59(2)
$d = 3$	SP	0.376	0.44(2)

different cases are gathered in Table III. In the case of the Hilhorst-van Leeuwen model the quality of the existing data do not allow a reliable determination of X_1^∞ for $x_1 > 3/4$. The main message of Table III is that X_1^∞ depends on the surface scaling dimension: for the Hilhorst-van Leeuwen model a variation in the strength of the defect amplitude A changes the value of X_1^∞ , whereas in the three-dimensional Ising model the different universality classes yield a different value for this limiting value. Assigning an effective local temperature via the equation $T_{eff} = T_c/X_1^\infty$, one has to remark that (a) the surface effective temperature in general differs from the effective temperature T_c/X_1^∞ inside the bulk, and (b) the surface effective temperature depends on the surface quantities (as for example the strength of the surface couplings) which determine the different surface universality classes.

VI. CONCLUSION AND OUTLOOK

The aim of the present work has been to extend the analysis of aging processes in critical systems far from equilibrium to the semi-infinite geometry, paying special attention to the behaviour of surface quantities in the dynamical scaling regime. As shown in the preceding Sections, surface autocorrelation and autoresponse functions display in this aging regime a scaling behaviour similar to that observed in the bulk, but with exponents differing from those encountered inside the bulk. This scaling behaviour has been investigated numerically in the two- and three-dimensional semi-infinite Ising models as well as in the Hilhorst-van Leeuwen model. The latter model is a semi-infinite two-dimensional Ising model with an extended surface defect which has the property that the surface scaling dimension varies continuously as a function of the defect amplitude. It is this property that has made possible a systematic study of the effects of surfaces on aging processes.

It is remarkable that the scaling functions of the surface thermoremanent magnetization are found to agree with the analytical predictions coming from the theory of local scale invariance.¹⁴ This extends the range of ap-

plicability of this theory to semi-infinite systems. At this stage field-theoretical computations of scaling functions are called for. Remembering the situation in the bulk systems, one may expect that renormalization group calculations also yield corrections to the predicted behaviour (22) in semi-infinite systems. This (expected) discrepancy between the observed agreement of the numerical data with the theoretical prediction on the one hand and the appearance of correction terms in a field-theoretical treatment on the other hand is an open problem which warrants more attention in the future.

Similar to what has been done in the bulk systems,¹³ field theoretical calculations should also permit to compute the limiting value X_1^∞ of the surface fluctuation-dissipation ratio. The dependence of X_1^∞ on the surface scaling dimension, as found in this work, again illustrates that the limiting value of the fluctuation-dissipation ratio permits to characterize the different (surface) universality classes.

Possible extensions of the present work include the study of nonequilibrium semi-infinite systems in cases where the order parameter is conserved (Kawasaki dynamics).²³ One would then be dealing with the semi-infinite extension of model B (in the classification of Hohenberg, Halperin and Ma), whereas in this work only the semi-infinite extension of model A has been considered. Indeed, the study of semi-infinite critical systems evolving with Kawasaki dynamics gives rise to new questions. It has been shown that in the semi-infinite extension of model B with a conserved bulk order parameter the presence of nonconservative surface terms, leading to a non-conserved local order parameter in the vicinity of the surface, yields a different dynamic critical universality class as compared to the case where these terms are absent. These two universality classes share the same critical exponents but are characterised by different scaling functions of equilibrium dynamic surface susceptibilities.^{37,53} It is therefore tempting to ask whether this different surface universality classes also show up when studying nonequilibrium quantities. Especially, it would be interesting to investigate the scaling functions of the autoresponse in these cases and to compare them with the prediction (22). A second obvious extension would be the study of semi-infinite systems at temperatures below T_c where phase-ordering takes place. Dynamical scaling behaviour is also observed in bulk systems in the low temperature phase and a similar behaviour is also expected for semi-infinite systems. Work along the sketched lines is planned for the future.

Acknowledgments

I thank Malte Henkel and Ferenc Iglói for inspiring discussions. The numerical work has been done on the IBM supercomputer Jump at the NIC Jülich (project Her10) and on the IA32 cluster of the Regionales Rechenzentrum Erlangen. I also acknowledge support by the Bayerisch-

Französisches Hochschulzentrum through a travel grant.

APPENDIX

In this Appendix I derive the expression (22) for the scaling function of the surface autoresponse under the assumption that local scale invariance¹⁴ holds. I hereby closely follow the derivation of the scaling function of the bulk autoresponse given in Ref. 14.

Consider the local two-point function $\mathcal{R}_1(t, s; \vec{\rho}_1, \vec{\rho}_2)$ which describes the response of the system at time t at the surface site $\vec{\rho}_1$ to a perturbation acting at time s at the surface site $\vec{\rho}_2$. As we are considering aging systems, time translation invariance is broken. However we still have space translation invariance along the surface, and therefore $\mathcal{R}_1(t, s; \vec{\rho}_1, \vec{\rho}_2) = \mathcal{R}_1(t, s; \vec{\rho})$ with $\vec{\rho} = \vec{\rho}_1 - \vec{\rho}_2$. We furthermore require that \mathcal{R}_1 transforms covariantly under scale (X_0) and special conformal (X_1) transformations, i.e. $X_0 \mathcal{R}_1 = X_1 \mathcal{R}_1 = 0$, where the differential operators X_0 and X_1 are explicitly given in Ref. 14. The differential equations for the surface autoresponse $R_1(t, s) = \mathcal{R}_1(t, s; \vec{0})$ are obtained by setting $\rho = |\vec{\rho}| = 0$, yielding

$$(t \partial_t + s \partial_s + \zeta_1 + \zeta_2) R_1(t, s) = 0 \quad (\text{A.1})$$

$$(t^2 \partial_t + s^2 \partial_s + 2\zeta_1 t + 2\zeta_2 s) R_1(t, s) = 0 \quad (\text{A.2})$$

with the solution

$$R_1(t, s) = r_0 \left(\frac{t}{s} \right)^{\zeta_2 - \zeta_1} (t - s)^{-(\zeta_1 + \zeta_2)} \Theta(t - s). \quad (\text{A.3})$$

Here, ζ_1 and ζ_2 are two exponents left undetermined by the theory, whereas r_0 is a normalization constant and Θ the step function. The exponents ζ_1 and ζ_2 are fixed by comparing expression (A.3) with the expected scaling behaviour (13) and (14), leading to the final result:

$$R_1(t, s) = r_0 \left(\frac{t}{s} \right)^{1+2x_1/z-\lambda_1/z} (t - s)^{-1-2x_1/z} \Theta(t - s). \quad (\text{A.4})$$

This can be written in the form

$$R_1(t, s) = s^{-1-2x_1/z} f_{R_1}(t/s) \quad (\text{A.5})$$

where the scaling function $f_{R_1}(y)$ is given by the expression (22).

-
- ¹ C. Godrèche and J.-M. Luck, J. Phys.: Condens. Matter **14**, 1589 (2002).
² L.F. Cugliandolo, in *Slow Relaxation and non equilibrium dynamics in condensed matter*, Les Houches Session 77 July 2002, J-L Barrat, J Dalibard, J Kurchan, M V Feigel'man eds (Springer, 2003).
³ A. Crisanti and F. Ritort, J. Phys. A **36**, R181 (2003).
⁴ A.J. Bray, Adv. Phys. **43**, 357 (1994).
⁵ L.F. Cugliandolo, J. Kurchan, and G. Parisi, J. Physique I **4**, 1641 (1994).
⁶ A. Barrat, Phys. Rev. **E57**, 3629 (1998).
⁷ L. Berthier, J.L. Barrat, and J. Kurchan, Eur. Phys. J. **B11**, 635 (1999).
⁸ C. Godrèche and J.M. Luck, J. Phys. A **33**, 1151 (2000).
⁹ C. Godrèche and J.M. Luck, J. Phys. A **33**, 9141 (2000).
¹⁰ E. Lippiello and M. Zannetti, Phys. Rev. E **61**, 3369 (2000).
¹¹ M. Henkel, M. Pleimling, C. Godrèche, and J.-M. Luck, Phys. Rev. Lett. **87**, 265701 (2001).
¹² L. Berthier, P.C.W. Holdsworth, and M. Sellitto, J. Phys. A **34**, 1805 (2001).
¹³ P. Calabrese and A. Gambassi, Phys. Rev. B **65**, 066120 (2002); Phys. Rev. E **66**, 066101 (2002).
¹⁴ M. Henkel, Nucl. Phys. **B641**, 405 (2002).
¹⁵ A. Picone and M. Henkel, J. Phys. A **35**, 5575 (2002).
¹⁶ P. Mayer, L. Berthier, J.P. Garrahan, and P. Sollich, Phys. Rev. E **68**, 016116 (2003).
¹⁷ F. Sastre, I. Dornic, and H. Chaté, Phys. Rev. Lett. **91**, 267205 (2003).
¹⁸ M. Henkel and J. Unterberger, Nucl. Phys. **B660**, 407 (2003).
¹⁹ M. Henkel, M. Paeßens, and M. Pleimling, Europhys. Lett. **62**, 664 (2003); Phys. Rev. E **69**, 056109 (2004).
²⁰ M. Henkel and M. Pleimling, Phys. Rev. E **68**, 065101(R) (2003).
²¹ G.F. Mazenko, Phys. Rev. E **69**, 016114 (2004).
²² S. Abriet and D. Karevski, Eur. Phys. J. B **37**, 47 (2004).
²³ C. Godrèche, F. Krzakala, and F. Ricci-Tersenghi, J. Stat. Mech.: Theor. Exp. P04007 (2004).
²⁴ A. Picone and M. Henkel, Nucl. Phys. B **688**, 217 (2004).
²⁵ C. Chatelain, cond-mat/0404017.
²⁶ S. Abriet and D. Karevski, cond-mat/0405598.
²⁷ D.A. Huse, Phys. Rev. **B40**, 304 (1989).
²⁸ H.K. Janssen, B. Schaub, and B. Schmittmann, Z. Phys. **B73**, 539 (1989).
²⁹ L.F. Cugliandolo, J. Kurchan, and L. Peliti, Phys. Rev. E **55**, 3898 (1997).
³⁰ M. Henkel and G. Schütz, J. Phys. A **37**, 591 (2004).
³¹ C. Chatelain, J. Phys. A **36**, 10739 (2003).
³² H.W. Diehl, Int. J. Mod. Phys. B **11**, 3503 (1997).
³³ M. Pleimling, J. Phys. A **37**, R79 (2004).
³⁴ H.J. Hilhorst and J.M. van Leeuwen, Phys. Rev. Lett. **47**, 1188 (1981).
³⁵ F. Iglói, I. Peschel, and L. Turban, Adv. Phys. **42**, 683 (1993), and references therein.
³⁶ S. Dietrich and H.W. Diehl, Z. Phys. B **51**, 343 (1983).
³⁷ H.W. Diehl, Phys. Rev. B **49**, 2846 (1994).
³⁸ H.W. Diehl, M. Krech, and H. Karl, Phys. Rev. B **66**, 024408 (2002).
³⁹ U. Ritschel and P. Czerner, Phys. Rev. Lett. **75**, 3882 (1995).
⁴⁰ S.N. Majumdar and A.M. Sengupta, Phys. Rev. Lett. **76**,

- 2394 (1996).
- ⁴¹ M. Kikuchi and Y. Okabe, Phys. Rev. Lett. **55**, 1220 (1985).
 - ⁴² H. Riecke, S. Dietrich and H. Wagner, Phys. Rev. Lett. **55**, 3010 (1985).
 - ⁴³ M. Pleimling and F. Iglói, Phys. Rev. Lett. **92**, 145701 (2004).
 - ⁴⁴ K. Binder and D.P. Landau, Phys. Rev. Lett. **52**, 318 (1984).
 - ⁴⁵ C. Ruge, A. Dunkelmann, and F. Wagner, Phys. Rev. Lett. **69**, 2465 (1992); C. Ruge, A. Dunkelmann, F. Wagner, and J. Wulf, J. Stat. Phys. **73**, 293 (1993).
 - ⁴⁶ H.W.J. Blöte and H.J. Hilhorst, Phys. Rev. Lett. **51**, 2015 (1983).
 - ⁴⁷ P.C. Hohenberg and B.I. Halperin, Rev. Mod. Phys. **49**, 435 (1977).
 - ⁴⁸ H.W. Diehl and H.K. Janssen, Phys. Rev. A **45**, 7145 (1992).
 - ⁴⁹ M. Henkel, A. Picone, and M. Pleimling, cond-mat/0404464.
 - ⁵⁰ A.J. Bray, J. Phys. A **23**, L67 (1990).
 - ⁵¹ A.J. Bray and B. Derrida, Phys. Rev. E **51**, R1633 (1995).
 - ⁵² M. Henkel, Adv. in Solid State Phys. **44** (2004) (in press) and cond-mat/0404016.
 - ⁵³ F. Wichmann and H.W. Diehl, Z. Phys. B **97**, 251 (1995).